Cell Wall Fracture Mechanism in Ultrasonic Assisted Cutting of Honeycomb Materials

Baohua Yu
Sufang Yao
Xin Wu
Xiaoping HU (xiaoping.hu@hdu.edu.cn)
Hangzhou Dianzi University

Research Article

Keywords: Ultrasonic cutting, honeycomb composites, thin plate theory, fracture characteristic

Posted Date: October 22nd, 2021

DOI: https://doi.org/10.21203/rs.3.rs-994724/v1

Cell Wall Fracture Mechanism in Ultrasonic Assisted Cutting of Honeycomb Materials

Baohua Yu[1] • Sufang Yao[1] • Xin Wu[1] • Xiaoping Hu[1]

Abstract
Revealing the ultrasonic cutting mechanism of honeycomb composite is important for determining the acoustic parameters of the ultrasonic system and selecting the parameters of the cutting process. Understanding more details of the stress on the cell wall from ultrasonic vibrating tool and the conditions for cell wall breakage is essential to study the machining mechanism. According to the evolution of contact state between the straight edge cutter and the honeycomb cell wall in a cycle, the cutting force acting on the cell wall is divided into three stages: transverse cutting load action, longitudinal cutting load action, and no cutting load action. The cell wall deflection and stress equations under transverse cutting load were established by applying elastic thin plate small deflection theory. The deformation and fracture characteristics of the honeycomb cell wall were analyzed by combining the analytical and the finite element model. The results showed that the ultrasonic vibration of the cutter greatly improved the stiffening effect of the cell wall and its fracture was caused by the deflection under the transverse cutting load, which exceeded the maximum allowable deformation after local stiffening. In addition, with only longitudinal cutting load, it was difficult to break the critical buckling state that leads to cell wall fracture.

Keywords: Ultrasonic cutting, honeycomb composites, thin plate theory, fracture characteristic

1 Introduction

Ultrasonic assisted machining is a non-traditional method that applies ultrasonic vibrations to the tool or workpiece along a certain direction during the machining process. It reduces the cutting force and cutting heat, improves the surface processing quality of the workpiece and enhances the processing efficiency [1].

The absorbing honeycomb material is prepared from regular hexagonal aramid paper used as the matrix, followed by impregnating the cell wall with resin mixed with acetylene carbon black as the absorbent [2]. It has all the characteristics and advantages of the aramid honeycomb material, such as lightweight, high strength-to-density ratio, high stiffness-to-density ratio, good self-extinguishing performance, and excellent insulation. In addition, the thicker impregnated layer could absorb wave to achieve stealth. Now the absorbing honeycomb materials have led to the widespread use in aerospace and other fields, and the scope of its application is still continuously progressing.

Conventional high-speed milling aramid honeycomb material has several drawbacks, including rough surface quality, low processing efficiency, and related health issues due to the dust chips. Recently, ultrasonic vibration assisted (UVA) processing have been considered more efficient for aramid honeycomb composites because of high surface precision, less tool and lower surface defects [3]. A lot of studies on the ultrasonic cutting of aramid honeycomb materials have been reported. Hu et al. [4] established the cutting force theoretical model and verified that vibration amplitude influence greatly on cutting force and surface quality with theory and experiments. Huang et al. [5] the fracture mechanics theory to study the micro-fracture process in honeycomb composites during ultrasonic cutting. Wang et al. [6] discussed the relative motion relationship between the straight edge cutter and the cell wall of the Nomex honeycomb material and established the dynamic force model of ultrasonic cutting based on brittle fracture mechanics. Similarly, following the characteristics of ultrasonic cutting with a straight edge cutter, Xiang et al. [7] studied the effects of cutting parameters on machined surface quality of honeycomb core wall, and verified that the slide effect caused by ultrasonic vibrations can reduce cutting resistance compared with ordinary cutting. Zhang et al. [8] adopted rip cutting, oblique cutting, and cross-cutting separately to cut the Nomex honeycomb materials and observed the morphology of the materials, and studied the influence of process parameters of the straight edge cutter on the damaged morphology. Kang et al. [9] analyzed the influence of processing parameters on cutting and surface quality based on the theoretical model and optimized the processing parameters via experimental investigations.

However, the components and thickness of the impregnation layer of the absorbing honeycomb material are different from that of the aramid honeycomb composites, and ultrasonic processing makes the absorbing honeycomb different defects such as significant breakage or even partial peeling appeared in the cell wall. The ultrasonic cutting process parameters suitable for the aramid honeycomb materials do not apply to cutting the absorbing honeycomb materials. Fewer reports on the mechanism of ultrasonic cutting for absorbing honeycomb materials considering the material properties exist, and the studies on the fracture process of the materials during ultrasonic cutting are also rare. A thorough understanding of the ultrasonic machining mechanism in the absorbing honeycomb materials would help to optimize the process parameters and promote the application of the ultrasonic cutting technology to other similar materials.

In the present study, the fracture mechanism of ultrasonic cutting of the absorbing honeycomb material was studied by investigating its cell wall. Firstly, based on the

✉ Xiaoping Hu
xiaoping.hu@hdu.edu.cn

[1] School of Mechanical Engineering, Hangzhou Dianzi University, Hangzhou 310018, China

analysis of the relative motion and contact force between the cutter and the material in a cycle, it was proposed that the cutting fracture in the cell wall might be caused either by the transverse cutting force or the longitudinal cutting force. Then, targeting the effect of the transverse cutting force, the deflection and stress equations for the honeycomb cell wall were established based on the theory of thin plate fracture mechanics. Also, the conditions that resulted in cell wall fracture were analyzed. The effect of the longitudinal cutting force on the cell wall stability was derived from the buckling theory. Finally, the feasibility of analyzing the cutting mechanism based on the small-deflection thin plate theory was discussed theoretically as well through simulations. The entire study was done on AC-AHM absorbing honeycomb material. This research provides theoretical guidance for expanding the applications of the ultrasonic machining technology for similar materials and expeditiously determining the plausible cutting process parameters.

2 Ultrasonic cutting process of the honeycomb cell wall with a straight edge cutter

2.1 Motion analysis of the straight edge cutter in ultrasonic cutting

The length, height, and width of the honeycomb materials were taken along the X, Y, and Z-axis, respectively. The straight edge cutter cut the honeycomb material with a feed speed of V_e along the Z-axis. In the meantime, the cutter vibrated ultrasonically along the axial direction. The relative position of the cutter and the material is given in Fig. 1.

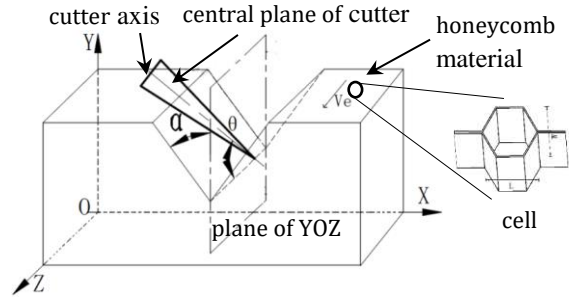

Fig. 1 Relative motion position of the honeycomb material and a straight edge cutter

To improve the holding stability and processing efficiency of the honeycomb material during processing, the central plane of the cutter was deflected relative to the YOZ plane, forming a cutter deflection angle α. In the meantime, the cutter axis was rotated within the central plane, resulting in a cutter inclination angle θ *b*etween the cutter axis and the direction of the speed. When the central plane of the cutter was further deflected at an angle of-α relative to the YOZ plane in one feed, a V-shaped chip was formed. This cutting method is called V-shaped cutting. Besides, the rectangular cutting method is commonly used to simplify numerical control programming further. Specifically, the deflection angle of the straight edge cutter was set at α=0^0. Once the cutter made cuts for two times with a specific spacing, the cutting disc then also cut the bottom, thereby forming the rectangular chip. Fig. 2 displays the relative position of the straight edge cutter and honeycomb cell wall in the rectangular cutting.

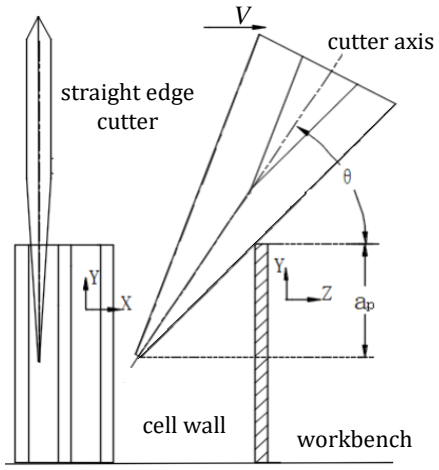

Fig. 2 The position of the straight edge cutter relative to the absorbing honeycomb cell wall when the cutter deflection angle is equal to 0^0

As mentioned above, in absorbing honeycomb material the impregnated layer consists of a resin mixed with the acetylene carbon black absorbent. Therefore, its out-of-plane stiffness is much greater than that of the Nomex honeycomb material. Hence, for the same vertical cutting depth, V-shaped cutting exerts more surface pressure on the straight edge cutter and has greater contact friction than rectangular cutting, thereby making the cutter more susceptible to wear or even fracture. Thus, rectangular cutting is more suitable for the processing of absorbing honeycomb materials.

In the process of ultrasonic cutting, the cutting motion of the straight edge cutter relative to the cell wall results from the longitudinal ultrasonic vibration of the cutter along the cutter axis and its feed motion along the Z direction. The cutting displacement and the speed in the three coordinate directions are given by equation (1.1)& (1.2):

$$\begin{cases} S_x = 0 \\ S_y = A\sin\theta \cdot \sin(2\pi f t) \\ S_z = A\cos\theta \cdot \sin(2\pi f t) + V_e t \end{cases} \tag{1.1}$$

$$\begin{cases} V_x = 0 \\ V_y = A\sin\theta \cdot 2\pi f \cdot \cos(2\pi f t) \\ V_z = A\cos\theta \cdot 2\pi f \cdot \cos(2\pi f t) + V_e \end{cases} \tag{1.2}$$

where A is the amplitude of the ultrasonic wave, f is the ultrasonic frequency, S is the motion displacement of the cutter, V is the cutter speed, and V_e is the speed along the feed direction of the cutter.

When $V_e < A\cos\theta \cdot 2\pi f$, the straight edge cutter and the material meet intermittently along the feed direction. The movement trajectory of the straight edge cutter is shown in Fig. 3. From Fig. 3 and equation (1.1) & (1.2), equation (1.3)can be obtained as follows:

$$\begin{cases} A\cos\theta \cdot 2\pi f \cdot \cos(2\pi f t_1) + V_e = 0 \\ S_z^1 = A\cos\theta \cdot \sin(2\pi f t_1) + V_e t_1 \\ S_z^2 = A\cos\theta \cdot \sin(2\pi f t_2) + V_e t_2 = S_z^1 \\ t_3 = t_1 + \frac{1}{f} \end{cases} \tag{1.3}$$

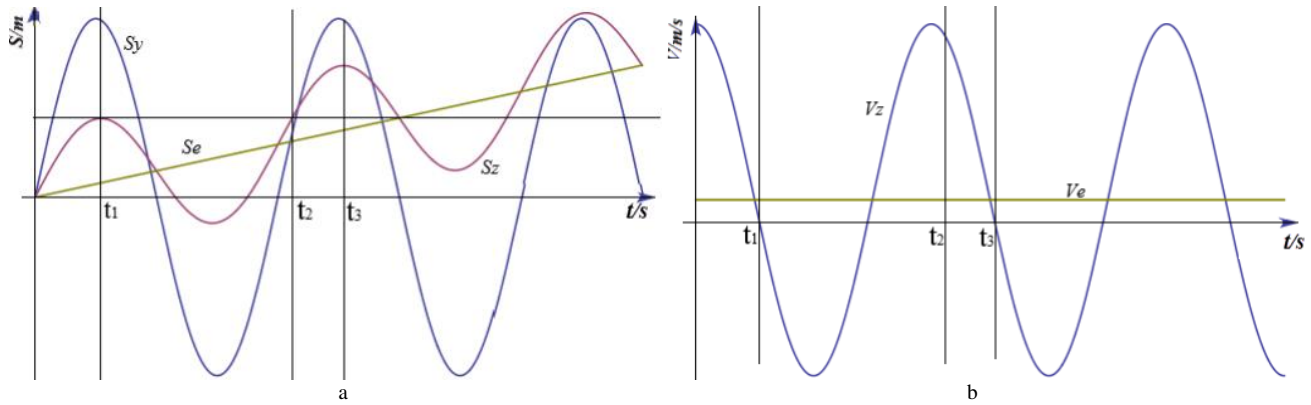

a b

Fig. 3 Displacement and speed curves of the straight edge cutter(a. Displacement curve, b. Speed curve)

where t_1 is the time when the straight edge cutter cuts at the deepest position S_z^1 along the feed direction in the first cycle. Also, t_1>T/4 according to Fig. 3. t_2 represents the time at, which the cutter exits the material and returns to S_z^1 to cut again and t_3 is when the cutter cuts through to the next deepest part. The cutting process further repeats from t_1 to t_3.

2.2 Evolution of the cutting force exerted on the honeycomb cell wall

The displacement trajectory of the cutting edge during the process is shown in Fig. 4. The variation of the cutting force acting on honeycomb cell wall with the time t for the straight edge cutter in one cycle is explained as below:

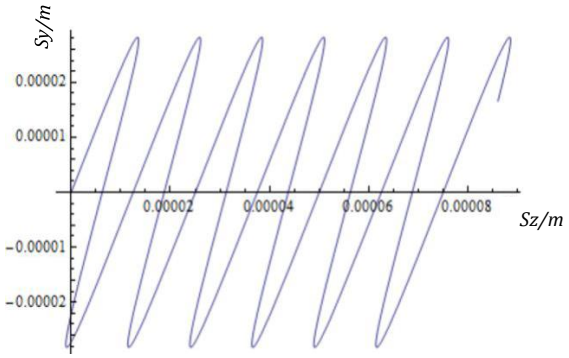

Fig. 4 The trajectory of the straight edge cutter in the honeycomb cell wall. (A = 30 μm, f = 20 kHz, θ= 70^0, and Ve = 15 m/min)

(1) 0 < t < T/4: During this time interval, the straight edge cutter pushes and presses the honeycomb cell wall in the Z direction, gradually increasing the cell wall deformation due to the effect of the transverse cutting load F_z. Along the Y direction, the cutter moves away from the cell wall; hence, there is no pressing of the cell wall from the longitudinal cutting load F_y.

(2) T/4 < t < t_1: The straight edge cutter exerts pressure on the honeycomb cell wall in both the Z and Y directions, resulting in the transverse cutting load F_z and the longitudinal cutting load F_y. However, during this extremely short period, the deformation of the cell wall due to F_y along the Y-direction is very small, thus, the impact of the longitudinal cutting load F_y can be neglected.

(3) t_1 < t < 3T/4: The direction of the motion of the straight edge cutter along the Z-axis is opposite to the feed direction, without exerting the transverse cutting load on the cell wall. However, the cutter presses against the cell wall in the Y direction, causing a pressing effect due to the longitudinal cutting load F_y. Also, with the increase in the displacement of the cutter along the Y-direction, the corresponding load on the cell wall grows accordingly.

(4) 3T/4 < t < t_2: Between this interval, the straight edge cutter moves away from the material in the Y direction and closer to the cell wall in the Z direction, although it does not reach the deepest position of the previous cycle. Now, the cutter does not exert any cutting force on the cell wall in either direction.

(5) t_2 < t < t_1+T: At this point, the cell wall and the straight edge cutter once again make a contact only in the Z direction, thereby repeating the process of (1).

The above observations indicated that the cell wall encountered three different situations in one ultrasonic vibration cycle: single Z-direction cutting load, single Y-direction cutting load, and no cutting load in any direction. This further analyzes the possibility of the fracture in the cell wall resulting from the single transverse or longitudinal cutting load.

3 Fracture of the honeycomb cell wall under the influence of the transverse cutting load F_z

The cell wall of the AC-AHM absorbing honeycomb material is a three-layered plate structure of absorbing resin–aramid paper–absorbing resin. The aramid matrix as the core layer is very thin relative to the whole cell wall and the cutting quality should be such that the three-layer structure remains intact or breaks as a whole without spalling off the absorbing impregnation layer. Therefore, the three-layer structure is regarded as an equally thick and homogeneous thin plate without considering the laminating effect of the cell wall. The cell structure of the absorbing honeycomb is shown in Fig. 5 and the corresponding length (l) and cell wall thickness (δ) are equal to 2.75 mm and 0.2 mm, respectively.

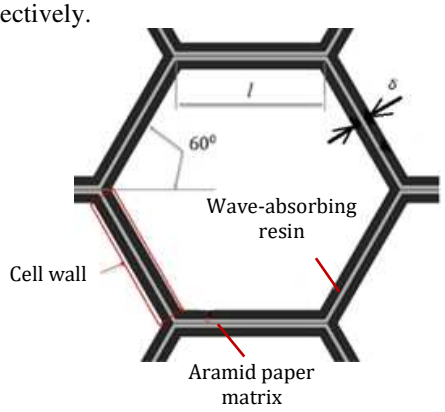

Fig. 5 The cell structure of the absorbing honeycomb material

Assuming that $1/80< \delta/l<1/5$ and also, the height of the honeycomb core workpiece is typically far larger than the cell wall thickness, hence the cell wall can be considered equivalent to a thin plate. The stress-strain curve obtained by Roy et al. [10] from the tensile test of the matrix cell wall material showed that the honeycomb cell wall exhibits strict linear elastic behavior before failure. Compared with the assuming condition in Timoshenko's book [11] the bending theory of an elastic thin plate with small deflection can be used to analyze the stress deformation and fracture in the absorbing honeycomb cell wall while getting cut with a straight edge cutter.

3.1 Cell wall deformation under the influence of transverse cutting load

Fig. 6 shows the simplified thin plate structure of the absorbing honeycomb cell wall. b is the length of the thin plate, corresponding to the height of the cut part of the cell wall of the honeycomb material, l represents the width of the thin plate, i.e., the side length of the cell, and δ is the thin plate thickness, implying the cell wall thickness.

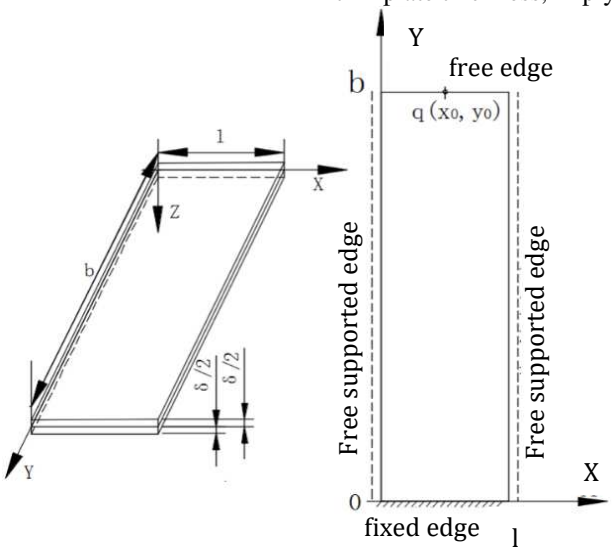

Fig. 6 Simplified thin plate structure of the absorbing honeycomb cell wall

When the absorbing honeycomb material was processed with ultrasonic cutting, the bottom of the material was fixed on the work table with a strong double-sided adhesive tape. Thus, the bottom of the cell wall can be considered as a fixed boundary. The two sides of the honeycomb cell wall were then supported by the two cell walls of the adjacent cells. When the stiffness of the honeycomb cell is sufficient, the two sides of the cell wall can be simply considered as the supported boundaries. Besides, the top of the cell wall is a free boundary, which is impacted by the cutter load during the process of cutting.

Considering the middle plane of the thin plate as the XY plane, the Z-direction deflection of the thin plate $\omega(x, y)$ satisfies the following boundary conditions:

$$\begin{cases} \omega|_{y=0} = 0 \\ \omega|_{x=0} = 0 \\ \omega|_{x=l} = 0 \\ \frac{\partial \omega}{\partial y}|_{y=0} = 0 \end{cases} \tag{1.4}$$

According to the Rayleigh-Ritz method, the deflection satisfying the boundary conditions can be expressed as:

$$\omega = C_1 (\frac{y}{b})^2 sin\frac{\pi x}{l} \tag{1.5}$$

where C_1 is an unknown quantity that needs to be solved.

Based on the principle of virtual displacement, the bending strain energy acting on the thin plate is given by equation (1.6):

$$U = \int_0^b \int_0^l \frac{D}{2} \left\{ \left(\frac{\partial^2 \omega}{\partial x^2} + \frac{\partial^2 \omega}{\partial y^2} \right)^2 - 2(1-\mu) \left[\frac{\partial^2 \omega}{\partial x^2} \cdot \frac{\partial^2 \omega}{\partial y^2} - \left(\frac{\partial^2 \omega}{\partial x \partial y} \right)^2 \right] \right\} dxdy \tag{1.6}$$

where D is the bending stiffness of the thin plate with a theoretical value of $D = \frac{E\delta^3}{12(1-\mu^2)}$, E is the elasticity modulus of the thin plate, and μ is the Poisson's ratio.

substituting equation (1.5) into equation (1.6), gives equation (1.7),

$$U = {C_1}^2 \cdot H \tag{1.7}$$

where $H = \frac{D}{2} \cdot \left[\frac{2l}{b^3} + \frac{b\pi^4}{10l^3} + \frac{4\pi^2 - 6\pi^2\mu}{3bl} \right]$.

When the transversely uniform force q acts on the thin plate, the bending deformation occurs in the Z direction, and the work done is given by equation (1.8):

$$W_z = \iint q\omega dxdy \tag{1.8}$$

When the cutting load F_z concentrated in the Z-direction acts on the cell wall at point (x_0, y_0), the transverse load can be replaced by the uniform load, $\frac{F_z}{dxdy}$ around the differential area of $dxdy$. Then, the differential area of q in equation (1.8) is equal to zero except at (x_0, y_0) where the differential area is equal to $\frac{F_z}{dxdy}$. Consequently, equation (1.8) can be rewritten as,

$$W_z = F_z \omega(x_0, y_0) \tag{1.9}$$

Putting equation (1.5)into equation (1.9), gives the following equation (1.10),

$$W_z = F_z \frac{{y_0}^2 sin[\frac{\pi x_0}{l}] C_1}{b^2} \tag{1.10}$$

The total potential energy of the cell wall is $\emptyset = U - W$. Taking advantage of the principle of least total potential energy $\frac{\partial \emptyset}{\partial C_1} = 0$, C_1 is obtained as:

$$C_1 = \frac{F_z {y_0}^2 sin[\frac{\pi x_0}{l}]}{2Hb^2} \tag{1.11}$$

By substituting C_1 into equation (1.5), the deflection formula for the wall cell is obtained as:

$$\omega = \frac{F_z {y_0}^2 sin[\frac{\pi x_0}{l}]}{2Hb^2}(\frac{y}{b})^2 sin\frac{\pi x}{l} \quad (1.12)$$

3.2 Cell wall fracture analysis under the influence of transverse cutting load

3.2.1 Cutting fracture based on stress intensity

According to the relationship between the stress and deflection of the thin plate along with the application of the transverse cutting load, the stresses σ_x, σ_y, and τ_{xy} for each point within the surface of the wall with thickness δ can be expressed as:

$$\sigma_x = z\frac{EC_1 sin[\frac{\pi x}{l}]}{b^2 l^2(1-\mu^2)}(\pi^2 y^2 - 2\mu l^2) \quad (1.13)$$

$$\sigma_y = z\frac{EC_1 sin[\frac{\pi x}{l}]}{b^2 l^2(1-\mu^2)}(\pi^2 y^2 \mu - 2l^2) \quad (1.14)$$

$$\tau_{xy} = z\frac{EC_1 cos[\frac{\pi x}{l}]}{b^2 l(1+\mu)}(-2\pi y) \quad (1.15)$$

While deducing the above Eqs, it is assumed that the straight edge cutter starts ultrasonic cutting by contacting the cell wall at a point in the middle of its upper edge $(\frac{l}{2}, b)$. As observed from equation (1.12), the deflection at this point is maximum on the whole cell wall, and is given by equation (1.16),

$$\omega' = \frac{F_z}{2H} \quad (1.16)$$

The in-plane stress on the cell wall is directly related to the deflection. The point $(\frac{l}{2}, b)$ has the largest deflection and thus the maximum in-plane stress.

On comparing the stresses of the point, it was found that $\sigma_x > \sigma_y, \tau_{xy} = 0$. Substituting equation (1.12), into equation (1.13), gives the principal stress of the point as,

$$\sigma_{xmax} = \frac{E\delta}{2(1-\mu^2)}\frac{\pi^2 b^2 - 2\mu l^2}{b^2 l^2}\frac{F_z}{2H} \quad (1.17)$$

This is also the maximum principal stress applied on the entire cell wall. When the maximum principal stress of a certain point in the thin plate reaches its threshold value, the thin plate fractures.

3.2.2 Cutting fracture based on deformation deflection

From the macroscopic point of view, when the deformation of the brittle and elastic honeycomb cell wall under the cutting force reaches its critical elastic deformation, the cell wall gets fractured.

Due to the thin-walled structure, the cell wall is prone to stress stiffening. Lin et al. [12] proposed that the higher the stress, the more significant is the stiffening effect. The in-plane stress varies at different positions of the cell wall. The point $(\frac{l}{2}, b)$ demonstrates the largest local stiffness on the entire cell wall, as the in-plane stress is largest at this position. The local stiffness D_0 and the theoretical bending stiffness D are interrelated, and Xie et al. [13] expressed the relation as: $D = kD_0(0 < k < 1)$ where k is the scaling factor.

Based on the theory of brittle fracture mechanics, when the amplitude along the feed direction of the straight edge cutter satisfies the condition of $Acos\theta > \frac{\lambda_0}{2}$, the cutter will cut the material intermittently, and the dynamic transverse cutting force of the cell wall would be given by equation (1.18):

$$F_z(t) = D_0[Acos\theta \cdot sin\, sin(2\pi ft) + V_e t - (Acos\theta - \lambda_0)] \quad (1.18)$$

where D_0 is the local stiffness of the cell wall, and λ_0 is the critical elastic deformation of the cell wall.

When the cell wall is constantly under the influence of the transverse cutting load between time 0 to t_1, the averaged transverse cutting force can be expressed as:

$$F_z = D_0\left[\lambda_0 - Acos\theta + \frac{V_e t_1}{2} + \frac{Acos\theta \cdot sinsin\,(\pi f t_1)^2}{\pi f t_1}\right] \quad (1.19)$$

The deflection ω' caused by the transverse load F_z is the elastic deformation of the cell wall. If it reaches the critical elastic deformation, i.e., $\omega' \geq \lambda_0$, the cell wall will experience a fracture. If the amplitude in the feed direction is equal to $Acos\theta$, the cell wall will be cut intermittently, and the maximum value of the critical elastic deformation ($\lambda_{0\,max}$) will be 2Acosθ.

Based on the above analysis, we could say that the cell wall undergoes a fracture under the influence of the transverse cutting force when,

$$\sigma_{xmax} > [\sigma], \text{ or } \omega' \geq 2Acos\theta$$

4 Fracture of the honeycomb cell wall under the influence of the longitudinal cutting load F_y

The small-deflection bending theory of the elastic thin plate was also used to analyze the fracture mechanism of the cell wall under the longitudinal cutting load F_y.

4.1 Critical longitudinal cutting force on the cell wall

The longitudinal cutting force F_y in the Y-direction buckles the cell wall and generates the mid-plane internal force F_{Ty}. The work done by the mid-plane force is given as:

$$W_y = -\int_0^b \int_0^{\frac{l}{2}} \frac{1}{2} F_{Ty}(\frac{\partial \omega}{\partial y})^2 dxdy \quad (1.20)$$

Since the cell wall is very thin, the longitudinal cutting load acting on the free boundary of the cell wall only generates the stress parallel to the middle plane, i.e., the plane stress σ_y' under the influence of the longitudinal cutting load is equal to:

$$\sigma_y' = -\frac{\int_0^l F_y dx}{l\delta} = -\frac{F_y}{\delta} \quad (1.21)$$

where δ is the cell wall thickness. The plane stress on the unit width of the cell wall results in the mid-plane internal force:

$$F_{Ty} = \delta\sigma_y' \quad (1.22)$$

On comparing equation (1.21) and (1.22), we obtained $F_{Ty} = -F_y$.

Besides, the amount of work done when the concentrated longitudinal cutting load F_y' acts on the point (x_0, y_0) of the cell wall is given as,

$$W_y = (\int_0^b \frac{1}{2} F_y'(\frac{\partial \omega}{\partial y})^2 dy) /_{(x=x_0)} = F_y' \frac{2sin^2[\frac{\pi x_0}{l}]C_1^2}{3b} \quad (1.23)$$

Similarly, by using the principle of least total potential energy, the critical longitudinal cutting load F_y' required to bend the cell wall is obtained as:

$$F_y' = \frac{3bH}{2sin^2[\frac{\pi x_0}{l}]} \quad (1.24)$$

4.2 The analysis of the cell wall fracture under the influence of longitudinal cutting load

The critical longitudinal cutting load required for bending at the middle point of the upper edge of the cell wall is given by equation (1.25),

$$F_y{}' = \frac{3bH}{2} \quad (1.25)$$

During this period, a friction component exists along the Z-direction between the straight edge cutter and the cell wall. In the case of a critical buckling state, even if the transverse force is very small, it is easy to break the equilibrium state, resulting in cell wall instability and fracture.Therefore, for the cell wall experiencing the longitudinal cutting force F_y, if the condition $F_y > F_y{}'$ is satisfied, the cell wall will fracture during the application of the longitudinal cutting load.

5 Empirical study of the mechanism of ultrasonic-assisted cutting method

The relevant parameters of the thin plate equivalent to the cell wall of the AC-AHM absorbing honeycomb are shown in Table 1. They are calculated according to the well-known theory from Gibson and Ashby [14], and revised by means of the approaches of virtual testing recommended by Seeman et al. [15].

Table 1 Relevant parameters of the equivalent thin plate.

Width (mm)	Length (mm)	Thickness (mm)	Elasticity modulus (Mpa)	Tensile strength （Mpa）	Density (Kg/m3)	Poisson's ratio
2.75	20	0.2	544	12.2	739.4	0.3

5.1 Local stiffening effect in ultrasonic cutting

According to the analysis done in section 3.2, the maximum critical elastic deformation is given by $\lambda_{0max} = 2Acos\theta$. Substituting this into equation (1.19) and (1.16) along with the condition required for the cell wall fracture i.e., $\omega^{'} \geq 2Acos\theta$, the local stiffness of the cell wall at the position can be obtained as:

$$D_0 \geq \frac{8\pi AHfcos\theta \cdot t_1}{2\pi Afcos\theta \cdot t_1 + \pi f V_e \cdot {t_1}^2 + 2Acos\theta \cdot sin(\pi f t_1)^2} \quad (1.26)$$

The corresponding process parameters of the ultrasonic cutting of AC-AHM absorbing honeycomb material are given in Table 2. Assuming that the honeycomb height or the panel length b is 20 mm, D_0 was calculated nearly $1.97\times 10^3\, N/m$. In the static case, the stiffness, D of the cell wall was about $4 \times 10^{-4}\, N/m$. It could be seen that $D_0 \gg D$, indicating that the ultrasonic vibration had a significant stiffening effect on the material.

Table 2 Process parameters in ultrasonic cutting with a straight edge cutter

Amplitude A (μm)	Frequency f (kHz)	Cutter inclination angle θ (^{0})	Cutter deflection angle α (^{0})	Feed speed Ve (m/min)	Cutting depth a_p (mm)
30	20	70	0	5	10

5.2 Calculation and subsequent verification of panel fracture

Between time 0 to t_1, the transverse cutting force increases with the increase in time. At t_1, the cutter exhibits the largest displacement in the feed direction. Besides, the cell wall also experiences maximum deflection and stress. The maximum principal stress and deflection of the cell wall under different cutting process parameters can be obtained from equation (1.3), (1.16), (1.17), and (1.19). The compared values of the strength limit and the maximum critical elastic deformation are shown in Table 3.

Table 3 Stress and deflection values of the cell wall under different process parameters of the ultrasonic cutting

A (m)	f (kHz)	θ (^{0})	V_e (m/min)	σ_{xmax} (Mpa)	$[\sigma]$ (Mpa)	$\omega^{'}$ (μm)	λ_{0max} (mm)
20	20	70	3	1.31	12.2	16.9	13.7
25	20	70	3	1.64		21.1	17.1
30	20	70	3	1.97		25.2	20.52
30	30	70	3	1.96		25.2	20.52
30	40	70	3	1.96		25.2	20.52
30	20	60	3	2.87		36.8	30
30	20	50	3	3.69		47.3	38.6
30	20	70	5	1.97		25.3	20.52
30	20	70	10	1.99		25.6	20.52
30	20	70	20	2.03		26	20.52

Under the influence of different ultrasonic cutting process parameters, the following condition is applicable,

$$\sigma_{xmax} < [\sigma], \text{ and } \omega^{'} \geq 2Acos\theta = \lambda_{0max}$$

In other words, the maximum principal stress in the panel does not reach the strength limit, but the deflection caused by the transverse cutting force exceeds the maximum critical elastic deformation in intermittent cutting.

By substituting the cell wall parameters listed in Table 1 into equation (1.25), the critical longitudinal cutting load under the buckling condition was $F_y{}' = 56.8N$. The honeycomb material was cut via a self-made experimental ultrasonic cutting machine by using different combinations of the process parameters. Fig. 7 shows the experimental ultrasonic cutting machine. The value of the cutting force measured by the Kistler-9119A

3D dynamometer was converted for a single cell wall. The corresponding longitudinal load exerted on the cell wall is shown in Table 4.

Table 4 Longitudinal load on the cell wall during ultrasonic cutting

No.	A Peak-to-peak value) (μm)	θ (^{0})	V_e (m/min)	F_y (N)
1	20	50	2	24.65
2	20	60	4	34.95
3	20	70	4.5	23.91
4	25	50	4	24.73
5	25	60	4.5	15.79
6	25	70	2	8.09
7	30	50	4.5	15.99
8	30	60	2	18.52
9	30	70	4	24.22

Fig. 7 Image of the process equipment used in the experiments

It was observed that the longitudinal load on the cell wall was less than 56.8N under different process parameters implying that $F_y < F_y{}'$. The longitudinal cutting force does not reach the critical value to destroy the buckling state of the panel, hence no fracturing of the cell wall.

The above calculations and experiments indicated that the local stiffness of the cell wall was greatly improved by the ultrasonic stiffening effect. The deflection generated by the relatively small transverse cutting force exceeds the critical elastic deformation which led to brittle fracture in the panel. At this moment, the tensile stress in the panel did not attain the strength limit, resulting in no tensile fracture. Besides, the longitudinal cutting force did not achieve the critical value required for the bending of the thin plate, not enough to cause a fracture in the cell wall.

6 Simulation studies for the fracture of the cell wall during ultrasonic cutting

6.1 Establishment of the simulation model

The ABAQUS simulation software was used to simulate the cutting of the AC-AHM absorbing honeycomb cell wall with a straight edge cutter. The initial contact point between the cutter and the cell wall was set at the midpoint of the upper edge of the cell wall. The relevant parameters of the cell wall are given in Table 1. Cemented carbide YG6X-1 was selected for the straight edge cutter and its basic performance parameters are shown in Table 5. Ultrasonic cutting process parameters are also shown in Table 2. Fig. 8 illustrates the simulation model. Free meshing and the C3D4 grid were used for the straight edge cutter, while sweep meshing and the C3D8R grid were adopted for the cell wall. The processed grid parts were assembled and oriented according to the position of the cutter and the material during the actual cutting. The load was defined by a periodic amplitude curve and expressed in the BC boundary. The boundary constraints on the cell wall were also set. In the meantime, the ultrasonic vibration cutting motion of the cutter was set by controlling the displacement and speed in the Y and Z directions, respectively. Finally, the simulations were run explicitly.

Table 5 Basic performance parameters of the straight edge cutter

Density (Kg/m3)	Elasticity modulus (Mpa)	Poisson's ratio
14500	400000	0.2

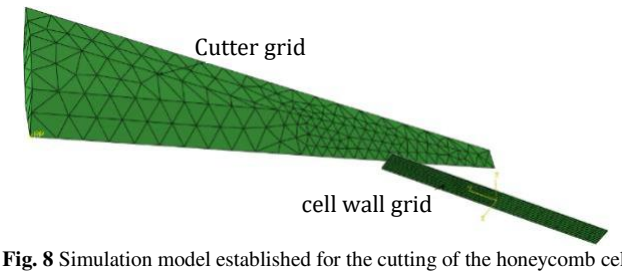

Fig. 8 Simulation model established for the cutting of the honeycomb cell wall by a straight edge cutter

6.2 Simulation of cell wall fracture process

The simulation results in Fig. 9 indicated that the cell wall was fractured at $t = 1.0 \times 10^{-5} s$.

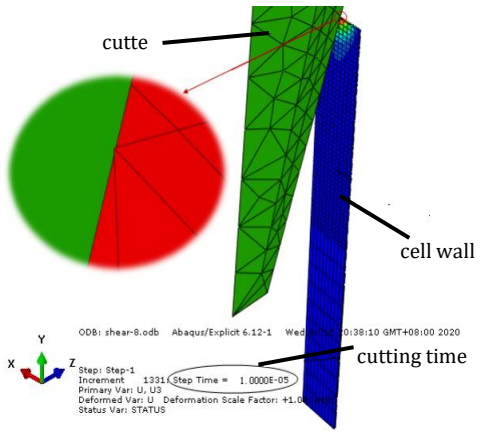

Fig. 9 Simulation results for the cell wall fracture

Also, the stress-time plot shown in Fig. 10, revealed that the stresses in the X and Y directions of the cell wall were much lower than the strength limit (12.2MPa). However, the deflection curve in Fig. 11 showed that the deformation in the cell wall was $21.8\mu m$, larger than the possible maximum critical elastic deformation λ_0 (20.5 μm). The simulation results were consistent with the theoretical analysis done in Section 4.2. Conclusively, we could say that the cell wall fracture was due to the deflection

deformation caused by the transverse cutting force. When the strength limit was used to control the fracture, the panel experienced a deformation much larger than $21.8\mu m$. This indicated that the ultrasonic vibration had a stiffening effect on the material, thereby, causing a brittle fracture in the cell wall.

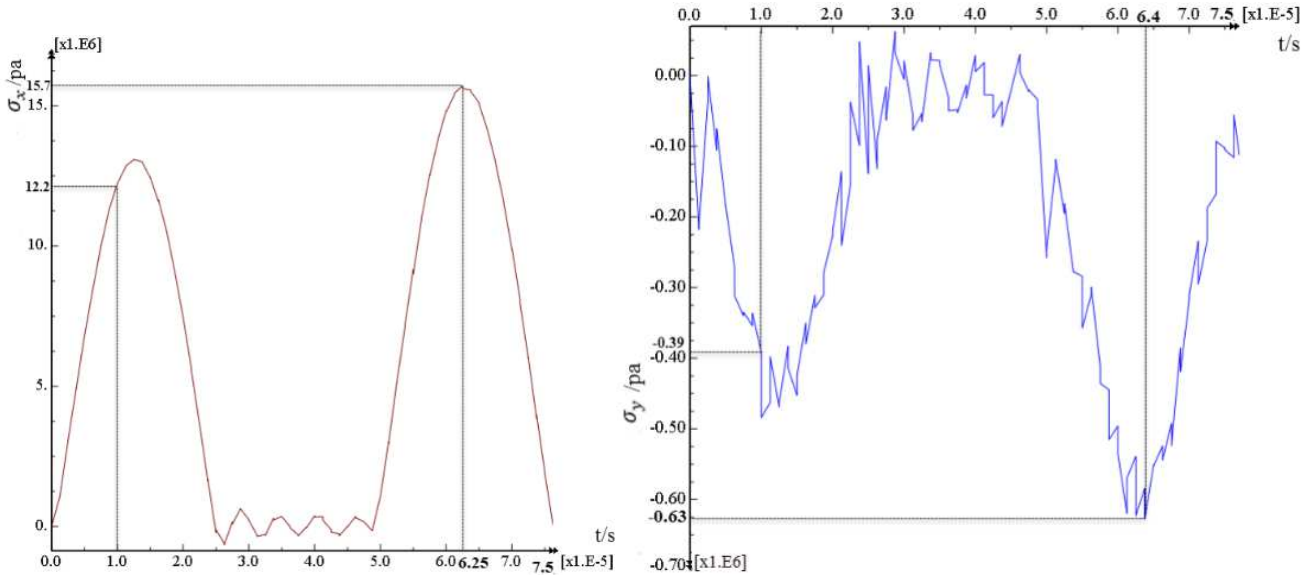

a b

Fig. 10 The in-plane stress-time plot of the cell wall(a. stress in X-direction, b. stress in Y-direction)

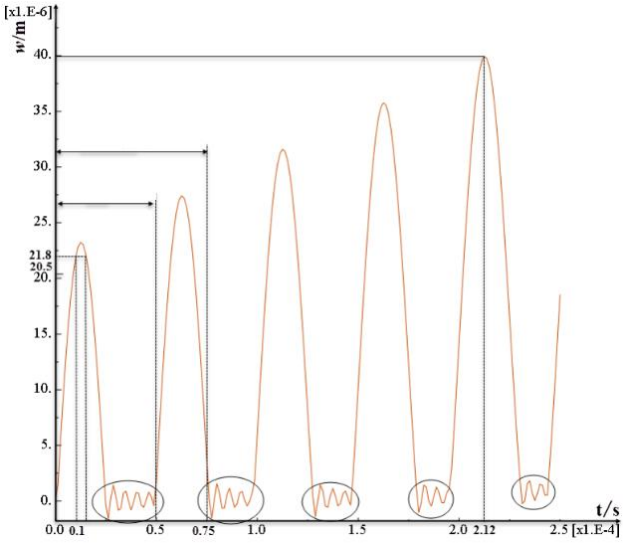

Fig. 11 Simulated deflection generated by the cell wall

Small deflection fluctuations were observed in the interval indicated by the circled part in Fig. 11. This was attributed to the inertial vibration in the thin plate once the cutter exited the cell wall.

7 Conclusions

The observations and the results of the study are summarized below:

(1) During one vibration cycle of the ultrasonic cutting, the cell wall experienced three different loading effects, including transverse cutting force, longitudinal cutting force, and no loading.

(2) The fracture of the cell wall is caused by transverse cutting force rather than longitudinal cutting force. The longitudinal cutting force was smaller than the critical longitudinal load on the cell wall in a buckling state, such that the cell wall could not be fractured. The contributing factor of fracture is the deflection caused by the transverse cutting force exceeds the maximum critical elastic deformation in intermittent cutting.

(3) The ultrasonic vibration exerted a stiffening effect on the material due to which the cell wall underwent a fracture even on the application of a small transverse cutting force. The fracture was brittle rather than a tensile fracture. This is more favorable to explain the presence of fewer defects of fiber pull-out on the fractured surface during ultrasonic cutting.

Author contribution: Baohua Yu comprehensively analyzed the simulation and data results, drew conclusions

and wrote part of the paper. Sufang Yao deduced the theoretical equation, did experiments, and wrote part of the paper. Xin Wu did simulation experiments. Xiaoping Hu designed and studied the technical route.

Funding: The National Natural Science Foundation of China (No.51975173), Zhejiang Province Public Welfare Technology Application Research Project (No. LGG21E050010),

Data availability: This article contains all the data gathered or analyzed during this study.

Ethical approval: None of the studies mentioned in this article contain any human participation. Also, no animals were harmed during these experiments.

Consent to participate: The authors consent to participate.

Consent for publication: The authors provide their consent to publish this article.

Competing interests: The authors declare no competing interests.

References

1. Ahmad, S., Zhang, J., Feng, P., Yu, D., Wu, Z., Ma, K., 2020. Processing technologies for Nomex Honeycomb Composites (NHCs): a critical review. Composite Structures. 250, 112545.
2. Cheng, W., Yuan, C., Qiu, Q., Wang, Q., Chen, J., 2015. Honeycomb sandwich structure and manufacturing process in aviation industry. Aeronautical Manufacturing Technology. 7, 94-98.
3. Gibson LJ, Ashby MF., 1988. Cellular solids: Structures & properties. Pergamon Press, Oxford.
4. Hu, X., Yu, B., Li, X., Chen, N., 2017. Research on cutting force model of triangular blade for ultrasonic assisted cutting honeycomb composites. In: Procedia CIRP. https://doi.org/10.1016/j.procir.2017.03.283.
5. Huang, X., Hu, X., Yu, B., Wu, S., 2015. Research on ultrasonic cutting mechanism of Nomex honeycomb composites based on fracture mechanics. Journal of Mechanical Engineering. 51, 205–212. https://doi.org/10.3901/JME.2015.23.205.
6. Kang D, Zou P, Wu H, Duan J, Wang W. 2019. Study on ultrasonic vibration–assisted cutting of Nomex honeycomb cores. The International Journal of Advanced Manufacturing Technology. 104, 979–992 https://doi.org/10.1007/s00170-019-03883-z.
7. Lin, J., Jin, S., Zheng, C., Yang, F., Ding, S., 2017. Variation analysis of accumulative stresses in multistep assembly processes using output transformation matrices. International Mechanical Engineering Congress and Exposition. 2, 1-13.
8. Roy, R., Park, S.-J., Kweon, J.-H., Choi, J.-H., 2014. Characterization of Nomex honeycomb core constituent material mechanical properties. Composite Structures. 117, 255-266.
9. Seemann, R., Krause, D., 2017. Numerical modelling of Nomex honeycomb sandwich cores at meso-scale level. Composite Structures. 159, 702-718.
10. Thoe, T. B., Aspinwall, D. K., Wise, M. L. H., 1998. Review on ultrasonic machining. Int. J. Mach. Tools Manufact. 38(4), 239-255.
11. Timoshenko, S.-P., 2009. Theory of elastic stability. Dover Publications Inc, New York.
12. Wang, Y., Wang, X., Kang, R., Sun, J., Jia, Z., Dong, Z., 2017. Analysis of influence on ultrasonic-assisted cutting force of nomex honeycomb core material with straight knife. Journal of Mechanical Engineering. 53, 73–82.
13. Xiang, D., Wu, B., Yao, Y., Zhao, B., Tang, J., 2019. Ultrasonic vibration assisted cutting of nomex honeycomb core materials. International Journal of Precision Engineering and Manufacturing. 20, 27-36.
14. Xie, S., Jing, K., Zhou, H., Liu, X., 2020. Mechanical properties of Nomex honeycomb sandwich panels under dynamic impact. Composite Structures. 235, 111814.
15. Zhang, X., Dong, Z., Wang, Y., Xu, Z., Song, H., Kang, R., 2017. Charization of surface microscopic of Nomex honeycomb after ultrasonic assisted cutting. Journal of Mechanical Engineering. 53, 90-99.